**Tian Z, Chen Z, Gong Y, Chambers JA.**

**Buffer-Aided Max-Link Relay Selection in Amplify-and-Forward Cooperative Networks.**

***IEEE Transactions on Vehicular Technology* 2015, 64(2), 553-565**

# Buffer-Aided Max-Link Relay Selection in Amplify-and-Forward Cooperative Networks

Zhao Tian, *Student Member, IEEE*, Gaojie Chen, Yu Gong, Zhi Chen, *Member, IEEE* and Jonathon Chambers, *Fellow, IEEE*

***Abstract*—This paper investigates the outage performance of an amplify-and-forward (AF) relay system which exploits buffer-aided max-link relay selection. Both asymmetric and symmetric source-to-relay and relay-to-destination channel configurations are considered. We derive the closed-form expressions for the outage probability, and analyze the average packet delays. We prove that the diversity order is between $N$ and $2N$ (where $N$ is the relay number), corresponding to a relay buffer size between $1$ and $\infty$ respectively. We also analytically show the coding gain. Numerical results are given to verify the theoretical analyse.**

***Index Terms*—Cooperative networks, relay selection, amplify-and-forward (AF), buffer-aided**

## I. Introduction

Relay selection can be applied in either non-regenerative (i.e. amplify-and-forward (AF)) or regenerative (i.e. decode-and-forward (DF)) relay systems [1]. The *max-min* relay selection is often considered as an optimum DF relay selection scheme, in which the best relay is selected with the highest gain among all of the minima of the source-to-relay and relay-to-destination channel gain pairs [2]. Although *max-min* schemes achieve diversity order of $N$ (where $N$ is the number of available relays), their performance is practically limited by the constraint that the best source-to-relay and relay-to-destination links for a packet transmission must be determined concurrently. Recent research has on the other hand found that, by introducing data buffers at the relays, this constraint can be relaxed to yield significant performance advantage in practical systems [3]–[10].

An early example of buffer-aided relay selection is the *max-max* scheme [6]. In max-max relay selection, at one time slot $t$, the best link among all source-to-relay channels is selected, and a data packet is sent to the selected relay and stored in the buffer. At the next time slot $t+1$, the best link among all relay-to-destination channels is selected, and the selected relay (which is often not the same relay selected at time $t$) forwards one data packet from its buffer to the destination. In this way, the strongest links from both source-to-relay and relay-to-destination group channels are always selected so that it has significant coding gain over the traditionary *max-min* scheme.

The *max-max* relay selection approach still follows the traditional transmission order in which the source-to-relay and relay-to-destination transmissions always carry on in an alternative manner, with a diversity order of $N$ which is the same as that for the *max-min* scheme. In the recent *max-link* approach [4], [8], this constraint on the transmission order is further relaxed so that, at any time, a best link is selected among all available source-to-relay and relay-to-destination links. Depending on whether a source-to-relay or a relay-to-destination link is selected, either the source transmits a packet to the selected relay or the selected relay forwards a stored packet to the destination. It is shown in [4] that the *max-link* relay selection not only has coding gain over the *max-min* scheme, but also has higher diversity order than both the *max-min* and *max-max* schemes. In particular, the diversity order can approach $2N$ when the relay buffer size is large enough.

While the buffer-aided relay selection describes a promising way forward in cooperative networks, existing approaches have been mainly for DF relay systems (e.g. [3]–[10]). This naturally prompts the following two questions:

- *Is it necessary or not to apply buffer-aided relay selection in an AF relay network?* In the AF system, the relay simply amplifies and forwards the received signal to the destination. Because the AF does not decode the received packets, it is not only easier to implement but also has higher level of security than a DF system [11]. When data buffers are applied at the relays, another difference between DF and AF is that alter "decoded digital data" or "received real signals" are stored in the buffers respectively. This brings up two implementation issues: quantization and data storage. It is interesting to point out that because the relay works in the half-duplex mode, that is it receives a data packet at one time slot and forwards it out at another slot, a data buffer (of size 1) actually exists even in the traditional AF or DF relay systems. In order to store the data in the buffer, quantization is always necessary for both AF and DF systems, no matter whether the buffers are used or not. Compared to its DF counterpart, therefore, buffer-aided AF relay selection has the extra implementation cost of storing quantized "real signals", but it retains the advantage of no decoding at the relays, making it particularly attractive in many applications such as mobile relays which are not always allowed to decode the source messages.



Z. Tian, G. J. Chen, Y. Gong and J. Chambers are with the Advanced Signal Processing Group, Loughborough University, Loughborough, Leicestershire, UK, Emails: { z.tian,g.chen,y.gong,j.a.chambers }@lboro.ac.uk.

Z. Chen is with the National Key Laboratory of Science and Technology on Communications, University of Electronic Science and Technology of China, Chengdu, Sichuan 611731, China, E-mail: chenzhi@uestc.edu.cn.

- *How is the buffer-aided relay selection applied in AF cooperative networks?* In traditional AF relay selection, the best relay is selected with the highest end-to-end signal-to-noise-ratio (SNR) at the destination [12], which is termed as the AF *max-SNR* scheme in this paper. When the AF relays are equipped with data buffers, however, the traditional max-SNR or its variants (e.g. [13]–[15]) cannot be used. This is because the source-to-relay and relay-to-destination links are selected separately which implies that the end-to-end SNR at the destination cannot be obtained instantaneously. In this paper, building upon traditional relay selection in DF relay selection schemes, such as the max-min scheme which may also be applied in an AF system (e.g. [16]), we propose to apply the DF max-link approach in the AF buffer-aided relay selection.

Of particular importance is the outage probability of the buffer-aided AF relay selection system. In a DF system, generally, the outage probability for the source-to-relay and relay-to-destination transmission can be obtained separately and then combined to give the overall outage probability. In contrast, the outage performance of an AF relay system depends on the probability distribution of the end-to-end SNR at the destination, making it usually harder to analyze than that of its DF counterpart. Particularly, as when a relay buffer is introduced in the AF relays, the best source-to-relay and relay-to-destination links for a packet transmission must be determined at different times, thus they are generally selected from different numbers of available links. As a result, the distribution of the end-to-end SNR no longer follows the form of the MacDonald distribution as in traditional AF *max-SNR* relay selection [12]. This makes the outage performance of the buffer-aided AF relay selection much more difficult to analyze than both the traditional max-SNR scheme and the buffer-aided DF max-link scheme. This is perhaps the main reason that AF buffer-aided relay selection has not been well studied.

In this paper therefore, buffer-aided AF max-link relay selection is carefully investigated. Unlike existing buffer-aided relay selection approaches (e.g. [3], [5], [7], [10]), this paper considers both symmetric and asymmetric channel configurations allowing the average gains for the source-to-relay and relay-to-destination channels to be different. Although the asymmetric channel assumption makes the analysis even more difficult, it represents a more practical scenario so that the results provide an important basis for new system design. The main contributions of this paper are summarized as follows:

- Analyzing the outage probability of the AF max-link scheme for both asymmetric and symmetric channel configurations. As far as we know, this is the first time asymmetric channels have been considered in buffer-aided relay selection, and the outage probability was been derived in closed-form for an AF buffer-aided relay selection scheme. Numerical simulations are used to verify the analyse. The results show that the outage performance gain of the AF max-link scheme over the traditional max-SNR scheme is more significant for symmetric channels. This gives important insight for designing buffer-aided relay systems: for example, power control at the source and relay nodes may be used to achieve symmetric channel configuration for better outage performance.
- Analyzing the average packet delays for both asymmetric and symmetric channels. The results show that when the relay-to-destination channels are stronger than the source-to-relay channels, the AF buffer-aided relay system introduces less delay. Therefore, the "best" delay and outage performance requires different channel conditions. This actually arises an interesting design topic for future study: how the delay and outage performance can be jointly optimised.
- Proving that the diversity order of the AF max-link relay selection scheme is between $N$ and $2N$ (where $N$ is the number of relays), and the lower and upper diversity limits are reached when the relay buffer size $L$ is 1 and $\infty$ respectively.
- Analytically showing the coding gain of the AF max-link scheme compared to the traditional AF max-SNR schemes.

The remainder of the paper is organized as follows: Section II describes buffer-aided AF max-link relay selection; Section III derives the closed-form expressions for outage probability; Section IV analyzes the average packet delay; Section V studies the diversity order; Section VI shows the coding gain; Section VII includes numerical simulations to verify the analyse; finally Section VIII summarizes and concludes the paper.

## II. AF MAX-LINK RELAY SELECTION

The system model of buffer-aided AF relay selection is shown in Fig. 1, where there is one source node ($S$), one destination node ($D$) and $N$ relay nodes ($R_k$, $1 \leq k \leq N$). All nodes operate in the half-duplex mode, that is they do not transmit and receive simultaneously. Each relay is equipped with a data buffer $Q_k$ ($1 \leq k \leq N$) of finite size $L$ (in the number of data packets). The data packets in the buffer obey the "first-in-first-out" rule.

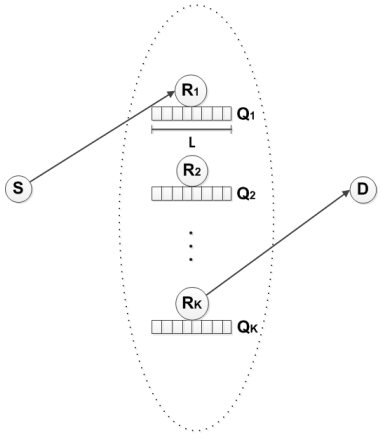


Fig. 1. The system model of the buffer-aided AF relay selection.

In this paper, we assume no direct transmission link between

the source and destination nodes[1]. We denote $h_{SR_k}(t)$ and $h_{R_kD}(t)$ as the frequency flat channel coefficients for $S \to R_k$ and $R_k \to D$ at time slot $t$ respectively. We assume all channel coefficients are independent and slowly Rayleigh fading such that they remain unchanged during one packet duration but independently vary from one packet time to another. The average $S \to R_k$ and $R_k \to D$ channel gains are assumed as

$$\mathrm{E}[|h_{SR_k}(t)|^2] = \sigma^2_{h_{sr}} \quad \mathrm{E}[|h_{R_kD}(t)|^2] = \sigma^2_{h_{rd}}, \text{for all } k, \quad (1)$$

respectively. We highlight that, while all channels for $S \to R_k$ and $R_k \to D$ are i.i.d. respectively, we do not assume symmetric channel configuration that is $\sigma^2_{h_{sr}} = \sigma^2_{h_{rd}}$. Without losing generality, we assume that the noise variances at all receiving nodes ($R_k$ and $D$) are the same. As in most existing relay selection approaches, we assume that the destination node has exact channel state information (CSI) for all channels so that it can choose the best relay node for transmission[2].

In max-link relay selection, the best transmission link is chosen with the highest channel SNR among all *available* source-to-relay and relay-to-destination links. A source-to-relay link is considered available when the buffer of the corresponding relay node is not full, and a relay-to-destination link is available when the corresponding relay buffer is not empty. If a source-to-relay link is selected, the source node transmits one data packet to the corresponding relay node, and the relay receives and stores the data packet in its buffer[3]. The number of data packets in the buffer is then increased by one. On the other hand, if a relay-to-destination link is selected, the corresponding relay transmits the earliest stored packet in the buffer to the destination, and the number of packets in the buffer is decreased by one. In general, the best selected relay node $R_{best}$ (for either reception or transmission) can be expressed as

$$R_{best} = \arg\max_{R_k} \left\{ \bigcup_{R_k:\Psi(Q_k)\neq L} \{|h_{SR_k}|^2\}, \bigcup_{R_k:\Psi(Q_k)\neq 0} \{|h_{R_kD}|^2\} \right\}, \quad (2)$$

where $\Psi(Q_k)$ gives the number of data packets in the buffer $Q_k$.

Without losing generality, at time slot $t$, we assume $S \to R_k$ is the strongest link so that the source transmits data packet $s(t)$ to the relay $R_k$. The received signal at $R_k$ is given by

$$y_{SR_k}(t) = \sqrt{E_s} h_{SR_k}(t) s(t) + n_{R_k}(t), \quad (3)$$

where $E_s$ is the average transmission power at the source and $n_{R_k}(t)$ is the additive-white-Gaussian-noise (AWGN) at $R_k$ with mean zero and variance $\sigma^2$.

Then $y_{SR_k}(t)$ is stored into the buffer $Q_k$ and waits for its turn to be transmitted. We assume that at the next $\tau$-th time slot, $y_{SR_k}(t)$ is forwarded from $R_k$ to the destination node. It is clear that $\Psi(Q_k(t)) \leq \tau < \infty$, where $\Psi(Q_k(t))$ gives the number of data packets in the buffer $Q_k$ at time $t$. Since the relays exploit AF, at the time slot $(t+\tau)$, the received signal at destination is given by

$$y_{R_kD}(t+\tau) = \sqrt{P_{R_k}(t+\tau)} h_{R_kD}(t+\tau) y_{SR_k}(t) + n_D(t+\tau), \quad (4)$$

where $n_D(t+\tau)$ is the noise at the destination node with mean zero and variance $\sigma^2$, and $P_{R_k}(t+\tau)$ is the relay gain at $R_k$ which is given by

$$P_{R_k}(t+\tau) = \frac{E_s}{E_s |h_{SR_k}(t)|^2 + \sigma^2}, \quad (5)$$

where we assume all relay nodes have the same average transmission powers as the source node, namely $E_s$.

Substituting (3) into (4) gives

$$\begin{aligned} y_{R_kD}(t+\tau) = \sqrt{E_s}\sqrt{P_{R_k}(t+\tau)} h_{R_kD}(t+\tau) h_{SR_k}(t) s(t) \\ + n_D(t+\tau) + n'_{R_k}(t), \end{aligned} \quad (6)$$

where $n'_{R_k}(t) = \sqrt{P_{R_k}(t+\tau)} h_{R_kD}(t+\tau) n_{R_k}(t)$.

We next derive the outage performance of the buffer aided AF relay system.

## III. Outage performance

The outage probability for the AF relay system can be defined as the probability that the instantaneous end-to-end SNR at the destination, $\gamma_D$, falls below a certain target SNR $\gamma_{th}$ such that

$$P_{out} = P(\gamma_D \leq \gamma_{th}), \quad (7)$$

where $P(\cdot)$ denotes the probability of an event. The Markov chain is used to model the transitions between the states of the buffers, where the states describe the number of data packets at every buffer [4]. There are $(L+1)^N$ states in total, and the $l^{th}$ state is expressed as

$$s_l = (\Psi(Q_1)\ \Psi(Q_2) \cdots \Psi(Q_N)), \quad l = 1, \cdots, (L+1)^N. \quad (8)$$

Suppose at time $t$, the state is at $s_j$. At time $t+1$, if a source-to-relay link is selected, a packet is transmitted to the selected relay and the number of packets in the corresponding data buffer is increased by 1. On the other hand, if a relay-to-destination link is selected, a packet in the selected relay is forwarded to the destination. Then at the destination, we assume that if the packet can be successfully decoded, it is stored at the destination, or otherwise is discarded[4]. In either case, the number of packets in the selected relay's buffer is decreased by 1. Thus depending on which relay receives or transmits data, at time $t+1$, the buffers may move from state $s_j$ to several possible states. We denote $\mathbb{A}$ as the $(L+1)^N \times (L+1)^N$ state transition matrix, where the entry $\mathbb{A}_{i,j} = P(X_{t+1} = s_i | X_t = s_j)$ which is the transition probability to move from state $s_j$ at time $t$ to state $s_i$ at time $(t+1)$.

We assume that when the data packet $s(t)$ is transmitted from the source to the destination through the best selected

[1]Including the direct link has little effect on the relay selection which is the main issue in this paper.

[2]While the CSI is normally estimated with pilot symbols or channels, this detail is beyond the scope of this paper.

[3]The received signal needs to be quantized before it is stored in the buffer. As was mentioned in the introduction, quantization exists in any half-duplex relaying, either AF or DF, with or without buffers. The quantization noise can either be ignored or absorbed in the channel noise.

[4]The discarded packet may need to be retransmitted. For example, in the TCP/IP protocol, the re-transmission is handled in the transport layer. The detailed implementation issue is beyond the scope of this paper.

relay $R_k$, the strongest source-to-relay and relay-to-destination links are selected when the buffer state is at $s_i$ and $s_j$ respectively. It then follows from (6) that, the instantaneous end-to-end SNR at the destination for receiving $s(t)$ is obtained as

$$\gamma_D^{(s_i,s_j)}(t+\tau) = \frac{\gamma_{SR_k}^{(s_i)}(t)\gamma_{R_kD}^{(s_j)}(t+\tau)}{\gamma_{SR_k}^{(s_i)}(t) + \gamma_{R_kD}^{(s_j)}(t+\tau) + 1}. \tag{9}$$

where $\gamma_{SR_k}^{(s_i)}(t)$ and $\gamma_{R_kD}^{(s_j)}(t+\tau)$ are the instantaneous SNRs for the $S \to R_k$ and $R_k \to D$ links at time $t$ and $t+\tau$ respectively, and the superscripts $^{(s_i)}$ and $^{(s_j)}$ denote that the corresponding best links are selected when the buffer state is at $s_i$ and $s_j$ respectively. Because we assume all channels at all times are independent fading, for clearer exposition, the time indices $t$ and $\tau$ are ignored unless otherwise necessary in the rest of the paper.

By considering all possible states for $s_i$ and $s_j$, the outage probability of the max-link AF relay selection is given by

$$P_{out} = \sum_{s_i}\sum_{s_j} P(s_i)P(s_j)P(\gamma_D^{(s_i,s_j)} < \gamma_{th}), \tag{10}$$

where $P(s_i)$ and $P(s_j)$ are the probabilities that the buffer state is at $s_i$ and $s_j$ respectively.

Below we show the derivation of $P(\gamma_D^{(s_i,s_j)} < \gamma_{th})$ and $P(s_i)$.

### A. $P(\gamma_D^{(s_i,s_j)} < \gamma_{th})$

We suppose at one time the strongest link is selected when the buffer state is at $s$. The buffer state $s$ uniquely corresponds to a pair of $\{K_{sr}^{(s)}, K_{rd}^{(s)}\}$, where $K_{sr}^{(s)}$ and $K_{rd}^{(s)}$ are the numbers of the available source-to-relay and relay-to-destination links respectively. Recall that a source-to-relay or relay-to-destination link is considered as "unavailable" if the buffer of the corresponding relay node is full or empty respectively.

Because all channels are assumed to be independently Rayleigh fading, the instantaneous SNR for every channel, $\gamma_w$ $(w \in \{SR_k, R_kD\})$, is independently exponentially distributed. Then based on the theory of order statistics [17], the cumulative distribution function (CDF) of the selected channel gain, $\gamma_w^{(s)}$, is given by

$$F_{\gamma_w^{(s)}}(x) = (1-e^{-\frac{x}{\bar{\gamma}_{sr}}})^{K_{sr}^{(s)}} \cdot (1-e^{-\frac{x}{\bar{\gamma}_{rd}}})^{K_{rd}^{(s)}}, w \in \{SR_k, R_kD\}, \tag{11}$$

where $\bar{\gamma}_{sr} = \frac{E_s\sigma_{h_{sr}}^2}{\sigma^2}$ and $\bar{\gamma}_{rd} = \frac{E_s\sigma_{h_{rd}}^2}{\sigma^2}$ which are the average SNR-s for the source-to-relay and relay-to-destination channels respectively. Differentiating (11) with respect to $x$ gives the probability density function (PDF) of $\gamma_w^{(s)}$ as

$$\begin{aligned} f_{\gamma_w^{(s)}}(x) = &\frac{K_{sr}}{\bar{\gamma}_{sr}} e^{-\frac{x}{\bar{\gamma}_{sr}}}(1-e^{-\frac{x}{\bar{\gamma}_{sr}}})^{K_{sr}-1}(1-e^{-\frac{x}{\bar{\gamma}_{rd}}})^{K_{rd}} \\ &+ \frac{K_{rd}}{\bar{\gamma}_{rd}} e^{-\frac{x}{\bar{\gamma}_{rd}}}(1-e^{-\frac{x}{\bar{\gamma}_{rd}}})^{K_{rd}-1}(1-e^{-\frac{x}{\bar{\gamma}_{sr}}})^{K_{sr}}, \end{aligned} \tag{12}$$

where $w \in \{SR_k, R_kD\}$.

Supposing the strongest source-to-relay and relay-to-destination links are selected when the buffer state is at $s_i$ and $s_j$ respectively, and because all channels are assumed to be mutually independent, we have

$$f_{\gamma_{SR_k}^{(s_i)}\gamma_{R_kD}^{(s_j)}}(x,y) = f_{\gamma_{SR_k}^{(s_i)}}(x) f_{\gamma_{R_kD}^{(s_j)}}(y), \tag{13}$$

Therefore

$$P(\gamma_D^{(s_i,s_j)} \le \gamma_{th}) = \iint\limits_{\frac{xy}{x+y+1}<\gamma_{th}} f_{\gamma_{SR_k}^{(s_i)}\gamma_{R_kD}^{(s_j)}}(x,y)\,dx\,dy, \tag{14}$$

which becomes (15) in the top of the next page.

Proof see Appendix.

### B. $P(s_i)$

Because the average channel gains for the $S \to R_k$ and $R_k \to D$ links are not the same, at any time the probabilities to select the source-to-relay and relay-to-destination transmission are also not the same. This is very different from existing buffer-aided relay selection schemes (e.g. the max-link approach in [4]) where the selection of any available link is equally likely. With this observation, we divide all states which can be moved from $s_l$ into two sets, $U_l^+$ and $U_l^-$, where $U_l^+$ contains all states to which $s_l$ can move when a source-to-relay link is selected and $U_l^-$ contains all states to which $s_l$ can move when a relay-to-destination link is selected. We let $p_{S\to R}^{(s_l)}$ and $p_{R\to D}^{(s_l)}$ be the probabilities that the source-to-relay and relay-to-destination transmissions are selected at state $s_l$, respectively. It is clear that $p_{S\to R}^{(s_l)} + p_{R\to D}^{(s_l)} = 1$.

On the other hand, because we assume all source-to-relay channels are i.i.d. fading and all relay-to-destination channels are also i.i.d. fading, the selection of one particular link within either $U_l^+$ or $U_l^-$ is equally likely. Therefore, the probabilities to select a source-to-relay or relay-to-destination link at state $s_l$ are given by

$$\begin{aligned} p_+^{(s_l)} &= \left(\frac{1}{K_{sr}^{(s_l)}} p_{S\to R}^{(s_l)}\right) = \frac{1}{K_{sr}^{(s_l)}}(1-p_{R\to D}^{(s_l)}), \\ p_-^{(s_l)} &= \left(\frac{1}{K_{rd}^{(s_l)}} p_{R\to D}^{(s_l)}\right) = \frac{1}{K_{rd}^{(s_l)}} p_{R\to D}^{(s_l)}, \end{aligned} \tag{17}$$

respectively.

With these observations, the $(i,j)$-th entry of the state transition matrix $\mathbb{A}$ is expressed as

$$\mathbb{A}_{i,j} = \begin{cases} p_+^{(s_j)} = \frac{1}{K_{sr}^{(s_j)}}(1-p_{R\to D}^{(s_j)}), & \text{if} \quad s_i \in U_j^+, \\ p_-^{(s_j)} = \frac{1}{K_{rd}^{(s_j)}} p_{R\to D}^{(s_j)}, & \text{if} \quad s_i \in U_j^-. \\ 0, & \text{elsewhere}, \end{cases} \tag{18}$$

Because the transition matrix $\mathbf{A}$ in (18) is column stochastic and irreducible[5], the stationary state probability vector is obtained as (see [20], [21])

$$\boldsymbol{\pi} = (\mathbf{A} - \mathbf{I} + \mathbf{B})^{-1}\mathbf{b}, \tag{19}$$

where $\boldsymbol{\pi} = [\pi_1, \cdots, \pi_{(L+1)^K}]^{\mathrm{T}}$, $\mathbf{b} = (1,1,...,1)^T$, $\mathbf{I}$ is the identity matrix and $\mathbf{B}_{n,l}$ is an $n \times l$ all unity element matrix. Or in the stationary state, we have $\pi_l = \lim_{t\to\infty} P(s_l)$ for $l = 1, \cdots, (L+1)^K$.

[5]*Column stochastic* means all entries in any column sum up to one, *irreducible* means that it is possible to move from any state to any state [19], [20].

$$P(\gamma_D^{(s_i,s_j)}<\gamma_{th}) = 1+\sum_{\substack{m\\(m,n)\neq(0,0)}}^{K_{sr}^{(s_i)}}\sum_{n}^{K_{rd}^{(s_i)}} C_{K_{sr}^{(s_i)}}^{m} C_{K_{rd}^{(s_i)}}^{n}(-1)^{m+n}2e^{-M_4\gamma_{th}}\sqrt{M_4 M_{\gamma_{th}}}\cdot$$
$$\cdot[\frac{K_{sr}^{(s_j)}}{\bar{\gamma}_{sr}}\sum_{a_1=0}^{K_{sr}^{(s_j)}-1}\sum_{a_2=0}^{K_{rd}^{(s_j)}}(-1)^{a_1+a_2}C_{K_{sr}^{(s_j)}-1}^{a_1}C_{K_{rd}^{(s_j)}}^{a_2}\frac{e^{-M_1\gamma_{th}}}{\sqrt{M_1}}\mathcal{B}(1,2\sqrt{M_1M_4M_{\gamma_{th}}}) \tag{15}$$
$$+\frac{K_{rd}^{(s_j)}}{\bar{\gamma}_{rd}}\sum_{a_3=0}^{K_{rd}^{(s_j)}-1}\sum_{a_4=0}^{K_{sr}^{(s_j)}}(-1)^{a_3+a_4}C_{K_{rd}^{(s_j)}-1}^{a_3}C_{K_{sr}^{(s_j)}}^{a_4}\frac{e^{-M_2\gamma_{th}}}{\sqrt{M_2}}\mathcal{B}(1,2\sqrt{M_2M_4M_{\gamma_{th}}})],$$

where

$$M_1=\frac{1}{\bar{\gamma}_{sr}}+\frac{a_1}{\bar{\gamma}_{sr}}+\frac{a_2}{\bar{\gamma}_{rd}}, M_2=\frac{1}{\bar{\gamma}_{rd}}+\frac{a_3}{\bar{\gamma}_{rd}}+\frac{a_4}{\bar{\gamma}_{sr}}, M_4=\frac{m}{\bar{\gamma}_{sr}}+\frac{n}{\bar{\gamma}_{rd}}, M_{\gamma_{th}}=\gamma_{th}(\gamma_{th}+1), \tag{16}$$

and $\mathcal{B}$ denotes the modified Bessel function of the second kind [18] and $C_M^N = M!/[N!(M-N)!]$ denotes the binomial coefficient.

Below we derive $p_{R\to D}^{(s_l)}$ in (18).

### C. $p_{R\to D}^{(s_l)}$: probability of selecting the relay-to-destination transmission at state $s_l$

If there are no relay-to-destination links available (or $K_{rd}^{(s_l)}=0$), we have $p_{R\to D}^{(s_l)}=0$. On the other hand, if there are no source-to-relay links available (or $K_{sr}^{(s_l)}=0$), we have $p_{R\to D}^{(s_l)}=1$. For other cases, $p_{R\to D}^{(s_l)}$ is given by

$$p_{R\to D}^{(s_l)} = P(x<y) = \int\int_{x<y} f_{XY}(x,y)dxdy, \tag{20}$$

where $x$ and $y$ are the maximum SNR-s from the $K_{sr}^{(s_l)}$ number of source-to-relay and $K_{rd}^{(s_l)}$ number of relay-to-destination links respectively, and $f_{XY}(x,y)$ is the joint PDF of $x$ and $y$. Because $x$ and $y$ are mutually independent, we have

$$\begin{aligned} f_{XY}(x,y) =& f_X(x)f_Y(y)\\ =&\frac{K_{sr}^{(s_l)}K_{rd}^{(s_l)}}{\bar{\gamma}_{sr}\bar{\gamma}_{rd}}e^{-(\frac{x}{\bar{\gamma}_{sr}}+\frac{y}{\bar{\gamma}_{rd}})}\cdot\\ &\cdot(1-e^{-\frac{x}{\bar{\gamma}_{sr}}})^{K_{sr}^{(s_l)}-1}(1-e^{-\frac{y}{\bar{\gamma}_{rd}}})^{K_{rd}^{(s_l)}-1}. \end{aligned} \tag{21}$$

where $f_X(x)$ and $f_Y(y)$ are the PDF-s of $x$ and $y$ respectively. Substituting (21) into (20), then we obtain the closed-form expression of $p_{R\to D}^{(s_l)}$ as (22) which is in the top of next page.

### D. A special case: symmetric $S\to R$ and $R\to D$ channels with $\sigma_{h_{sr}}^2=\sigma_{h_{rd}}^2$

In this section, we consider a special case that the average channel gains for the source-to-relay and relay-to-destination links are the same, or $\sigma_{h_{sr}}^2=\sigma_{h_{rd}}^2$. Under this symmetric channel scenario, the probabilities to select any available source-to-relay and relay-to-destination link at state $s_l$ at any time are the same. Thus (17) can be simplified as

$$p_{s_l}^+ = p_{s_l}^- = \frac{1}{K^{(s_l)}}, \qquad l=1,\cdots,(L+1)^N, \tag{23}$$

where $K^{(s_l)}=K_{sr}^{(s_l)}+K_{rd}^{(s_l)}$ which is the total number of available links (including both source-to-relay and relay-to-destination links) at state $s_l$. Then the state transition matrix is given by

$$\mathbb{A}_{i,j}=\begin{cases}\frac{1}{K^{(s_j)}}, & \text{if} \quad s_i\in U_j,\\ 0, & \text{elsewhere,}\end{cases} \qquad j=1,\cdots,(L+1)^N, \tag{24}$$

where $U_j$ is the set of all possible states to which can be moved from $s_j$ at the next time slot.

The stationary state probability vector is then obtained by substituting (24) into (19). Alternatively, because at any time the probability to select one available link is uniform and every link corresponds to one transition of states, the stationary probability for a state is proportional to its corresponding number of available links so that we have

$$\pi_j=\lim_{t\to\infty}P(s_j)=\frac{K^{(s_j)}}{\sum_{l=1}^{(L+1)^N}K^{(s_l)}}. \tag{25}$$

For the proof of (25) please refer to examples 1.9.6 and 1.9.7 in [20].

Next, we need to calculate the outage probability for the "symmetric" channel, $P_{out}^{\text{symmetric}}$, when the strongest source-to-relay and relay-to-destination links are selected at state $s_i$ and $s_j$ respectively. By letting $\bar{\gamma}=\bar{\gamma}_{sr}=\bar{\gamma}_{rd}$, and following the similar procedure in Section III-A, we can obtain the overall outage probability for the symmetric channel configuration as (26) in the top of the next page.

Next, we consider the average delay introduced in such networks

## IV. Average Packet Delay

In the AF max-link scheme, at a transmission node (either the source or a relay), a data packet can only be transmitted out if the corresponding link is selected. This brings up two issues: first, the packets may not arrive at the destination in order; second, each packet may suffer from different delay within the systems. While the first issue can be easily handled by for instance numbering every packet, the delay becomes a main issue in buffer-aided relay selection systems [9].

In general, a packet delay includes delays at both the source and selected relay nodes, which are denoted as $D_s$ and $D_r$ respectively. A simple example is illustrated in Fig. 2, where there are three packets ($s(1), s(2)$ and $s(3)$) transmitted out

$$
\begin{aligned}
p_{R\to D}^{(s_l)} &= \int_0^{\infty}\int_0^{y} \frac{K_{sr}^{(s_l)}K_{rd}^{(s_l)}}{\bar{\gamma}_{sr}\bar{\gamma}_{rd}} e^{-(\frac{x}{\bar{\gamma}_{sr}}+\frac{y}{\bar{\gamma}_{rd}})}(1-e^{-\frac{x}{\bar{\gamma}_{sr}}})^{K_{sr}^{(s_l)}-1}(1-e^{-\frac{y}{\bar{\gamma}_{rd}}})^{K_{rd}^{(s_l)}-1}dxdy \\
&= \sum_{m=0}^{K_{rd}^{(s_l)}-1}\sum_{n=0}^{K_{sr}^{(s_l)}} C_{K_{rd}^{(s_l)}-1}^{m} C_{K_{sr}^{(s_l)}}^{n}(-1)^{m+n}\frac{K_{rd}^{(s_l)}\cdot\bar{\gamma}_{sr}}{\bar{\gamma}_{sr}+\bar{\gamma}_{sr}\cdot m+\bar{\gamma}_{rd}\cdot n}
\end{aligned} \tag{22}
$$

$$
\begin{aligned}
P_{out}^{\text{symmetric}} =& \sum_{s_i}\sum_{s_j}\frac{K^{(s_i)}}{\sum_{l=1}^{(L+1)^N}K^{(s_l)}}\cdot\frac{K^{(s_j)}}{\sum_{l=1}^{(L+1)^N}K^{(s_l)}}\left(1+\frac{K^{(s_j)}}{\bar{\gamma}}\sum_{n=0}^{K^{(s_j)}-1}\sum_{m=1}^{K^{(s_i)}}C_{K^{(s_j)}-1}^{n}C_{K^{(s_i)}}^{m}\cdot\right. \\
&\left.\cdot(-1)^{m+n}2e^{-\frac{\gamma_{th}}{\bar{\gamma}}(1+m+n)}\sqrt{\frac{m\gamma_{th}(\gamma_{th}+1)}{(n+1)}}\mathcal{B}\left(1,\frac{2}{\bar{\gamma}}\sqrt{m\gamma_{th}(\gamma_{th}+1)(n+1)}\right)\right).
\end{aligned} \tag{26}
$$

consecutively from the source. The transmission time-span for every packet is represented by a horizontal bar in Fig. 2, where $D_s$ and $D_r$ indicate the delay time slots at the source and relay nodes respectively, and $S-R$ and $R-D$ indicate the transmission time slots for source-to-relay and relay-to-destination respectively. For example, packet $s_1$ is transmitted from the source to a relay node at time slot 2. After that, packet $s_2$ waits for three time slots (slots 3, 4 and 5) and is then transmitted to a relay. After $s_2$ arrives at the relay at slot 6, it waits for another four time slots (slots 7-10) before it is eventually transmitted to the destination at slot 11. Thus the delays for $s_2$ at the source and relay nodes are 3 and 4 respectively in this example. Fig. 2 also shows that the packets arrive at the destination in the order of $[s_1, s_3, s_2]$, which is clearly not the same as the transmission order.

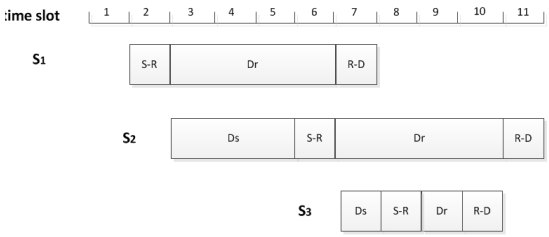


Fig. 2. An example of packet delay in the AF max-link scheme.

We particularly highlight that, while different packets may suffer from different delays, the system throughput (or the average data rate) of the AF max-link scheme is not scarified. This is because that, at any time slot, there is always one link selected for transmission. Therefore, when a packet is "waiting" for transmission at a node, another packet must be transmitted at another node. Assuming there are $M$ packets in total, as each packet takes two time slots for transmission (excluding the waiting time), if $M$ is large enough, the overall transmission time to deliver all packets is approximately $2M$. Therefore, the system average throughput is $\eta = \frac{M}{2M} = 0.5$, which is the same as that for the classic three-node "$S \to R \to D$" relay system [22].

According to Little's law [23], the average packet delay at the node $i$ can be obtained as

$$
\mathrm{E}[D_i] = \frac{\mathrm{E}[Q_i]}{\eta_i}, \tag{27}
$$

where $\mathrm{E}[Q_i]$ and $\eta_i$ are the average queuing length and throughput at the node.

In the following two subsections, we derive the average packet delay at the source and relay nodes respectively.

### A. Average packet delay at the source

Because all data are transmitted from the same source node, the average throughput at the source node is the same as that for the overall system which is given by

$$
\eta_s = \eta = 1/2 \tag{28}
$$

On the other hand, if we assume that the source always has data to transmit, the queuing length at the source depends on how fast the data leave the source, which again depends on the probability that a source-to-relay link is selected. Considering all buffer states at the relay, the probability that a source-to-relay link is selected can be obtained as $p_{S\to R} = \sum_{l=1}^{(L+1)^N}\pi_l \cdot p_{S\to R}^{(s_l)} = \sum_{s_l} P(s_l)\cdot(1-p_{R\to D}^{(s_l)})$, where $\pi_l$ is the stationary probability for state $s_l$ which is obtained in (19), and $p_{R\to D}^{(s_l)}$ is the probability to select a relay-to-destination link at state $s_l$ which is given by (22). Alternatively, for any fixed sized buffers, the number of data packets arriving at all the relays must be equal to that leaving these relays, because no data packet can stay in a relay node forever and fail to reach the destination. Thus we must have

$$
p_{S\to R} = p_{R\to D} = 1/2 \tag{29}
$$

This implies that the average queuing length at the source node is

$$
\mathrm{E}[Q_s] = 1/2 \tag{30}
$$

Substituting (28) and (30) into (27) gives the average packet delay at the source node as

$$
\mathrm{E}[D_s] = \frac{\mathrm{E}[Q_s]}{\eta_s} = 1. \tag{31}
$$

We highlight that (31) holds for both symmetric and asymmetric channel scenarios.

### B. Average packet delay at the relay

Because the probabilities to select any of the relays are the same, the average packet delays at any of the relay are also the same, so the average throughput at any relay is given by

$$\eta_r = \frac{\eta}{N} = \frac{1}{2N} \tag{32}$$

Let $Q_r^{(s_l)}$ be the queuing length (or the average number of packets) for the selected relay at the buffer state $s_l$. Considering all buffer states $s_l$, the average queuing length at the selected relay is obtained as

$$\mathrm{E}[Q_r] = \sum_{l=1}^{(L+1)^N} \pi_l Q_r^{(s_l)}, \tag{33}$$

Substituting (32) and (33) into (27) gives the average packet delay at the relay as

$$\mathrm{E}[D_r] = \frac{1}{2N} \sum_{l=1}^{(L+1)^N} \pi_l Q_r^{(s_l)} \tag{34}$$

Finally, combining the delay at the source and relay nodes gives the overall average delay in the AF max-link system as

$$\mathrm{E}[D] = \mathrm{E}[D_s] + \mathrm{E}[D_r] = 1 + \frac{1}{2N} \sum_{l=1}^{(L+1)^N} \pi_l Q_r^{(s_l)}. \tag{35}$$

On the other hand, if the source-to-relay and relay-to-destination channels are symmetric (i.e. $\sigma_{h_{sr}}^2 = \sigma_{h_{rd}}^2$), the average packet delay at the relay in (34) can be obtained as $\mathrm{E}[D_r] = L/2$, and the overall average delay becomes $\mathrm{E}[D] = 1 + NL$.

### C. Numerical examples

We have performed extensive numerical simulation which all well match the above delay analysis. Some of the results are shown in Tables I and II, where for fair comparison, we let $\bar{\gamma}_{sr}(\mathrm{dB}) + \bar{\gamma}_{rd}(\mathrm{dB}) = 40\mathrm{dB}$ in all cases. It is clearly shown that, with increased relay number $N$ and larger buffer size $L$, we have larger delays. Moreover, if the relay-to-destination link SNR is stronger than the source-to-relay SNB, we have smaller delay. This is not surprising because higher relay-to-destination SNR implies that the relay-to-destination link is more likely to be selected and the data are more quickly forwarded to the destination.

TABLE I
AVERAGE PACKET DELAYS

| $(N, L) = (2, 2)$ | $D_{ave}$ | |
|---|---|---|
| $(\bar{\gamma}_{sr}, \bar{\gamma}_{rd})$ [dB] | Simulation | Theory |
| 10 30 | 2.03 | 2.03 |
| 15 25 | 2.29 | 2.29 |
| 20 20 | 4.99 | 5.00 |
| 25 15 | 7.69 | 7.70 |
| 30 10 | 7.97 | 7.97 |

We next consider the diversity order of the scheme.

## V. Diversity Order

In order to show the diversity order of the AF max-link scheme, we assume all channels are i.i.d. such that $\sigma_{h_{sr}}^2 = \sigma_{h_{rd}}^2 = \sigma_h^2$, and then the outage probability is given in (26). The diversity order can be defined as

TABLE II
AVERAGE PACKET DELAYS

| $(N, L) = (4, 4)$ | $D_{ave}$ | |
|---|---|---|
| $(\bar{\gamma}_{sr}, \bar{\gamma}_{rd})$ [dB] | Simulation | Theory |
| 10 30 | 2.04 | 2.04 |
| 15 25 | 2.42 | 2.42 |
| 20 20 | 17.04 | 17.00 |
| 25 15 | 31.56 | 31.57 |
| 30 10 | 31.95 | 31.95 |

$$r = -\lim_{\bar{\gamma}_h \to \infty} \frac{\log P_{out}}{\log \bar{\gamma}_h}, \tag{36}$$

where $\bar{\gamma}_h = (E_s \sigma_h^2)/\sigma^2$ which is the average SNR for every channel. However substituting (26) into (36) does not explicitly shows the diversity order. Instead, we first derive the upper and lower bounds of the outage probability, from which the diversity order is obtained; then we show that the minimum and maximum diversity orders are obtained when the relay buffer sizes are 1 and $\infty$ respectively.

### A. Outage probability bounds

Noting $\gamma_{SR_k}^{(s_i)} = \bar{\gamma}_h |h_{SR_k}|^2$, $\gamma_{R_k S}^{(s_j)} = \bar{\gamma}_h |h_{R_k D}|^2$, and from (9), we have

$$\lim_{\bar{\gamma}_h \to \infty} \gamma_D^{(s_i, s_j)} = \frac{\gamma_{SR_k}^{(s_i)} \gamma_{R_k D}^{(s_j)}}{\gamma_{SR_k}^{(s_i)} + \gamma_{R_k D}^{(s_j)}}. \tag{37}$$

Since $\gamma_{SR_k}^{(s_i)} > 0$ and $\gamma_{R_k D}^{(s_j)} > 0$, we have

$$\frac{1}{2}\min(\gamma_{SR_k}^{(s_i)}, \gamma_{R_k D}^{(s_j)}) \le \frac{\gamma_{SR_k}^{(s_i)} \gamma_{R_k D}^{(s_j)}}{\gamma_{SR_k}^{(s_i)} + \gamma_{R_k D}^{(s_j)}} \le \min(\gamma_{SR_k}^{(s_i)}, \gamma_{R_k D}^{(s_j)}). \tag{38}$$

From (37) and (38), we have

$$P_e^L \le \lim_{\bar{\gamma}_h \to \infty} P(\gamma_D^{(s_i, s_j)} < \gamma_{th}) \le P_e^U, \tag{39}$$

where $P_e^L = P(\min(\gamma_{SR_k}^{(s_i)}, \gamma_{R_k D}^{(s_j)}) < \gamma_{th})$ and $P_e^U = P(1/2 \cdot \min(\gamma_{SR_k}^{(s_i)}, \gamma_{R_k D}^{(s_j)})$ which are the lower and upper bounds for $\lim_{\bar{\gamma}_h \to \infty} P(\gamma_D^{(s_i, s_j)} < \gamma_{th})$ respectively.

Supposing the total numbers of available links for buffer state $s_i$ and $s_j$ are given by $K^{(s_i)}$ and $K^{(s_j)}$ respectively, the lower bound $P_e^L$ can be obtained as

$$\begin{aligned} P_e^L &= P(\min(\gamma_{SR_k}^{(s_i)}, \gamma_{R_k D}^{(s_j)}) < \gamma_{th}) \\ &= (1 - e^{-\frac{\gamma_{th}}{\bar{\gamma}_h}})^{K^{(s_i)}} + (1 - e^{-\frac{\gamma_{th}}{\bar{\gamma}_h}})^{K^{(s_j)}} \\ &\quad - (1 - e^{-\frac{\gamma_{th}}{\bar{\gamma}_h}})^{K^{(s_i)}} (1 - e^{-\frac{\gamma_{th}}{\bar{\gamma}_h}})^{K^{(s_j)}}. \end{aligned} \tag{40}$$

Further noting that $e^x \approx 1 + x$ for very small x, and ignoring the high order terms, we have

$$\lim_{\bar{\gamma}_h \to \infty} P_e^L = \left(\frac{\gamma_{th}}{\bar{\gamma}_h}\right)^{\min\{K^{(s_i)}, K^{(s_j)}\}}. \tag{41}$$

Then we have $-\lim_{\bar{\gamma}_h \to \infty} \frac{\log P_e^L}{\log \bar{\gamma}_h} = \min\{K^{(s_i)}, K^{(s_j)}\}$. Further noting that $N \le K^{(s_i)} \le 2N$ and $N \le K^{(s_j)} \le 2N$, we

have

$$N \leq -\lim_{\bar{\gamma}_h \to \infty} \frac{\log P_e^L}{\log \bar{\gamma}_h} \leq 2N. \tag{42}$$

On the other hand, the upper bound $P_e^U$ can be obtained as

$$\begin{aligned} P_e^U &= P(1/2 \cdot \min(\gamma_{SR_k}^{(s_i)}, \gamma_{R_k D}^{(s_j)}) < \gamma_{th}) \\ &= (1 - e^{-\frac{2\gamma_{th}}{\bar{\gamma}_h}})^{K^{(s_i)}} + (1 - e^{-\frac{2\gamma_{th}}{\bar{\gamma}_h}})^{K^{(s_j)}} \\ &\quad - (1 - e^{-\frac{2\gamma_{th}}{\bar{\gamma}_h}})^{K^{(s_i)}} (1 - e^{-\frac{2\gamma_{th}}{\bar{\gamma}_h}})^{K^{(s_j)}}, \end{aligned} \tag{43}$$

Then following the similar procedure as that for $P_e^L$, we have

$$\lim_{\bar{\gamma}_h \to \infty} P_e^U = \left(\frac{\gamma_{th}}{\bar{\gamma}_h}\right)^{\min\{K^{(s_i)}, K^{(s_j)}\}}, \tag{44}$$

and

$$N \leq -\lim_{\bar{\gamma}_h \to \infty} \frac{\log P_e^U}{\log \bar{\gamma}_h} \leq 2N. \tag{45}$$

It is clear from (41) and (44) that, when $\bar{\gamma}_h \to \infty$, $\log P_e^L$ and $\log P_e^U$ have the same gradients against $\log \bar{\gamma}_h$. Then using (42) and (45) in (39), we must have

$$N \leq -\lim_{\bar{\gamma}_h \to \infty} \frac{\log P(\gamma_D^{(s_i,s_j)} < \gamma_{th})}{\log \bar{\gamma}_h} \leq 2N. \tag{46}$$

Particularly, if $K^{(s_i)} = K^{(s_j)} = K$, we have

$$-\lim_{\bar{\gamma}_h \to \infty} \frac{\log P(\gamma_D^{(K,K)} < \gamma_{th})}{\log \bar{\gamma}_h} = K. \tag{47}$$

Finally, because (46) holds for every $s_i$ and $s_j$, from (10), the diversity order of the max-link AF relay selection can be obtained as

$$N \leq r \leq 2N. \tag{48}$$

It is clear that the diversity order $r$ is a function of both the relay number $N$ and buffer size $L$. Below we show the upper and lower limits of the diversity order are reached when $L = 1$ and $L \to \infty$ respectively.

### *B. Buffer size $L = 1$*

If the buffer size $L = 1$, the available number of links at any state is $N$, or we have $P(K^{(s_i)} = N) = 1$ for all $s_i$. Then from (10), the outage probability is given by

$$P_{out}^{(L=1)} = P(\gamma_D^{(N,N)} < \gamma_{th}). \tag{49}$$

Furthermore from (47), we have the diversity order for $L = 1$ as

$$r = -\lim_{\bar{\gamma}_h \to \infty} \frac{P_{out}^{(L=1)}}{\log \bar{\gamma}_h} = N. \tag{50}$$

### *C. Buffer size $L \to \infty$*

If the buffer size is $L$, there are $(L-1)^N$ states which are neither full nor empty so that their corresponding number of available links is $2N$. Since the total number of buffer states is $(L+1)^N$, the number of states whose corresponding links is not $2N$ is $(L+1)^N - (L-1)^N$. Thus the probability that the available link is not $2N$ is given by

$$P(K \neq 2N) = \sum_{K^{(s_j)} \neq 2N} \pi_j, \tag{51}$$

where $K^{(s_j)}$ and $\pi_j$ are the total number of available links and stationary probability for the state $s_j$ respectively. Substituting (25) into (51), and recalling that $N \leq K^{(s_j)} \leq 2N$ for all $j$, we have

$$\begin{aligned} P(K \neq 2N) &= \sum_{K^{(s_j)} \neq 2N} \frac{K^{(s_j)}}{\sum_{l=1}^{(L+1)^N} K^{(s_l)}} \\ &\leq \sum_{D_j \neq 2N} \frac{2N}{\sum_{l=1}^{(L+1)^N} N} = 2 \cdot \frac{(L+1)^N - (L-1)^N}{(L+1)^N - 1}. \end{aligned} \tag{52}$$

It is clear from (52) that $\lim_{L \to \infty} P(K \neq 2N) = 0$.

Therefore, if $L \to \infty$, the outage probability in (10) can be simplified as

$$P_{out}^{(L \to \infty)} = P(\gamma_D^{(2N,2N)} < \gamma_{th}). \tag{53}$$

Then from (47), we obtain the diversity order for $L \to \infty$ as

$$r = -\lim_{\bar{\gamma}_h \to \infty} \frac{P_{out}^{(L \to \infty)}}{\log \bar{\gamma}_h} = 2N. \tag{54}$$

Lastly, we analyse the coding gain of the approach.

## VI. Coding gain

Compared with the traditional max-SNR relay selection scheme, the AF max-link scheme has not only diversity but also coding gain. In order to highlight the coding gain, we assume the relay buffer size of the max-link scheme is $L = 1$. Then the diversity orders for both the max-link and max-SNR schemes are $N$, and the outage performance advantage of the AF max-link over the max-SNR scheme comes from the coding gain.

From (49), when $L = 1$, the outage probability of the AF max-link scheme is given by $P_{out}^{(L=1)} = P(\gamma_D^{(N,N)} < \gamma_{th})$ whose lower and upper bounds ($P_e^L$ and $P_e^U$ respectively) can be obtained using (39). As is shown in Section V-A, when the channel SNR $\bar{\gamma}_h \to \infty$, $\log P_e^L$ and $\log P_e^U$ have the same gradients against $\log \bar{\gamma}_h$. This implies that, for $\bar{\gamma}_h \to \infty$, we must have

$$10 \log P_{out}^{(L=1)} = \alpha + 10 \log P_e^L, \tag{55}$$

where $0 \leq \alpha \leq \log(P_e^U / P_e^L)$ which is a small constant.

Substituting (40) into (55), and ignoring the high order terms in the context of high SNR, we have

$$\lim_{\bar{\gamma}_h \to \infty} 10 \log P_{out}^{(L=1)} = \alpha + 10 \log \left(2 \cdot \frac{\gamma_{th}}{\bar{\gamma}_h}\right)^N \tag{56}$$

On the other hand, in the traditional max-SNR scheme, the best relay is selected that maximizes the SNR at the destination. To be specific, if the relay $R_k$ is selected, the end-to-end SNR at the destination can be obtained as

$$\gamma_D^{(R_k)} = \frac{\gamma_{SR_k} \gamma_{R_k D}}{\gamma_{SR_k} + \gamma_{R_k D} + 1}, \tag{57}$$

where $\gamma_{SR_k}$ and $\gamma_{R_k D}$ are the instantaneous channel SNRs for $S \to R_k$ and $R_k \to D$ links respectively. Similar to (39), we can obtain the lower and upper bounds for $P(\gamma_D^{(R_k)} < \gamma_{th})$ assuming high SNR as

$$\begin{aligned} P(\min(\gamma_{SR_k}, \gamma_{R_k D}) < \gamma_{th}) \leq P(\gamma_D^{(R_k)} < \gamma_{th}) \leq \cdot\cdot \\ \cdot\cdot \leq P(\frac{1}{2} \cdot \min(\gamma_{SR_k}, \gamma_{R_k D}) < \gamma_{th}). \end{aligned} \tag{58}$$

Because the best relay in the max-SNR scheme is selected among $N$ pairs of source-to-relay and relay-to-destination links that maximizes (57), the outage probability can be obtained as

$$P_{out}^{(max-SNR)} = [P(\gamma_D^{(R_k)} < \gamma_{th})]^N \tag{59}$$

Substituting (58) into (59) gives

$$\begin{aligned}[P(\min(\gamma_{SR_k}, \gamma_{R_k D}) < \gamma_{th})]^N \leq P_{out}^{(max-SNR)} \leq ..\\ .. \leq [P(\frac{1}{2} \cdot \min(\gamma_{SR_k}, \gamma_{R_k D}) < \gamma_{th})]^N.\end{aligned} \tag{60}$$

For the similar reasons in obtaining (55), at high SNR, we must have

$$10 \log P_{out}^{(max-SNR)} = \beta + 10 \log[P(\min(\gamma_{SR_k}, \gamma_{R_k D}) < \gamma_{th})]^N \tag{61}$$

where $\beta$ is a small positive constant. Because the channel SNRs are exponentially distributed, we have

$$\begin{aligned}&[P(\min(\gamma_{SR_k}, \gamma_{R_k D}) < \gamma_{th})]^N = \\ &\left((1 - e^{-\frac{\gamma_{th}}{\bar{\gamma}_h}}) + (1 - e^{-\frac{\gamma_{th}}{\bar{\gamma}_h}}) - (1 - e^{-\frac{\gamma_{th}}{\bar{\gamma}_h}})(1 - e^{-\frac{\gamma_{th}}{\bar{\gamma}_h}})\right)^N.\end{aligned} \tag{62}$$

Substituting (62) into (61), and ignoring the high orders assuming high SNR, we have

$$\lim_{\bar{\gamma}_h \to \infty} 10 \log P_{out}^{(max-SNR)} = \beta + 10 \log \left(2 \cdot \frac{\gamma_{th}}{\bar{\gamma}_h}\right)^N \tag{63}$$

Finally, from (56) and (63), when the buffer size $L = 1$, the coding gain of the AF max-link scheme over the traditional AF max-SNR scheme is given by

$$\begin{aligned}\theta^{(L=1)}(\text{dB}) &= \lim_{\bar{\gamma}_h \to \infty} \left(10 \log P_{out}^{(max-SNR)} - 10 \log P_{out}^{(L=1)}\right) \\ &= 10(N-1) \log 2 + (\beta - \alpha) \\ &\approx 10(N-1) \log 2,\end{aligned} \tag{64}$$

where the approximation in (64) comes from the fact that both $\alpha$ and $\beta$ are small positive constants.

We recall that data buffers (with size 1) also exist at the relays in a traditional relay selection scheme, as the data packets need to be stored in the relay at one time and forwarded to the destination at the next time. It is clear from (64) that, even with $L = 1$, the AF max-link scheme still has better outage performance than the traditional AF max-SNR scheme because of the coding gain. It is also shown in (64) that more relays lead to higher coding gain. Only when $N = 1$, does the coding gain disappear because then both the max-link and max-AF schemes reduce to the standard three nodes relay system.

While the coding gain analysis above is for buffer size $L = 1$, it is also useful in understanding the more general case with other buffer sizes, where the coding gain also exists. In general, the coding gain depends on the number of available links for selection, which again depends on both the relay number $N$ and buffer size $L$. With larger $L$ and $N$, we have larger coding gain. This will be verified in the simulations in the next section.

## VII. Simulations and Discussions

In this section, numerical results are shown to verify the analyse in this paper. In the simulations below, the average transmission powers for all transmission nodes is set as $E_s = 1$, the noise variances for all receiving nodes are set as $\sigma^2 = 1$. All simulation results are obtained with 1,000,000 Monte Carlo runs.

### A. Outage performance of the AF max-link scheme

Fig. 3 verifies the outage probability expression in (26) with simulation results under various scenarios. It is clearly shown that in all cases the theoretical analysis well matches the simulation results. Both Fig. 3 (a) and (b) show that the best outage performance is obtained when the source-to-relay and relay-to-destination channels are symmetric.

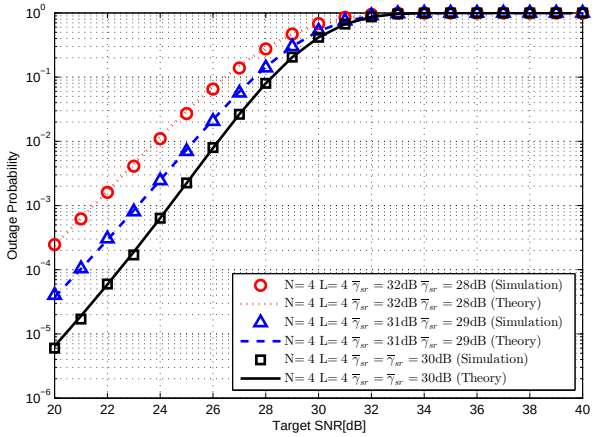


(a) $N = 4$, $L = 4$

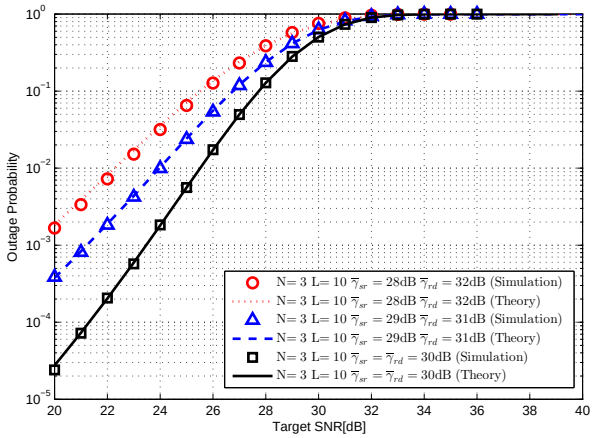


(b) $N = 3$, $L = 10$

Fig. 3. Outage probability performance of the AF max-link scheme: theory *vs* simulation.

Fig. 4 (a) and (b) show the outage performance against different buffer lengths $L$ for symmetric and asymmetric channel configurations respectively, where the relay number is fixed at $N = 3$. It is clearly shown that the outage performance improves with larger buffer size $L$, but the improvement is less significant when $L$ becomes larger. It is shown in Fig. 4 (a) and

(b) that, when $L = 50$ and $L = 20$, the outage performance is almost the same as that for $L \to \infty$ for the symmetric and asymmetric channel configurations respectively. Therefore, in practice, the full outage order $2N$ can be achieved with finite buffer sizes. It is also shown that, with larger buffer size $L$, the outage performance improvement in the symmetric channel (Fig. 4 (a)) is much more significant than that in the asymmetric channel (Fig. 4 (b)).

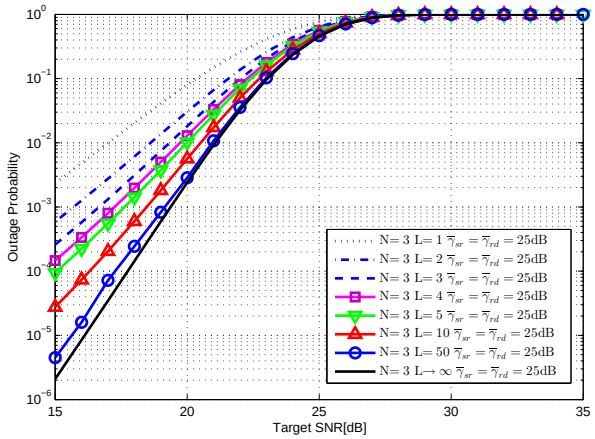


(a) Symmetric channels

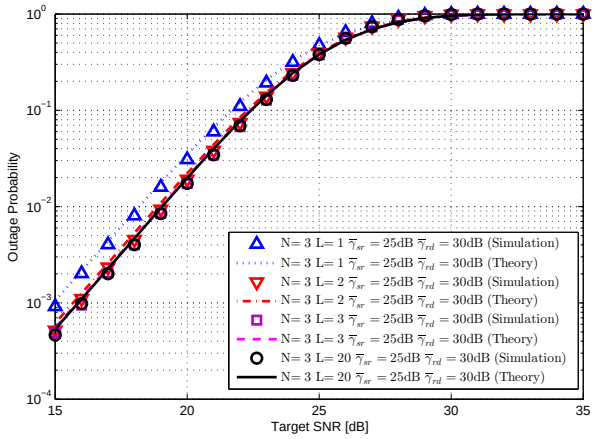


(b) Asymmetric channels

Fig. 4. Outage probability performance of the max-link scheme for different buffer lengths $L$.

Fig. 5 shows how the outage performance changes with different relay numbers $N$ for a fixed buffer size $L = 8$, where the asymmetric channel configuration with $\bar{\gamma}_{sr} = 30$dB and $\bar{\gamma}_{rd} = 25$dB is considered. It is clearly shown that the outage performance improves with more relays. The results for other channel configurations are similar so they are not presented.

### *B. Outage performance comparison between the AF max-link and max-SNR schemes*

Fig. 6 compares the proposed AF max-link and traditional max-SNR schemes in symmetric and asymmetric channels. For fair comparison, we let $\bar{\gamma}_{sr}(\text{dB}) + \bar{\gamma}_{rd}(\text{dB}) = 40$dB in all cases. It is clearly shown that, for both the AF max-link and

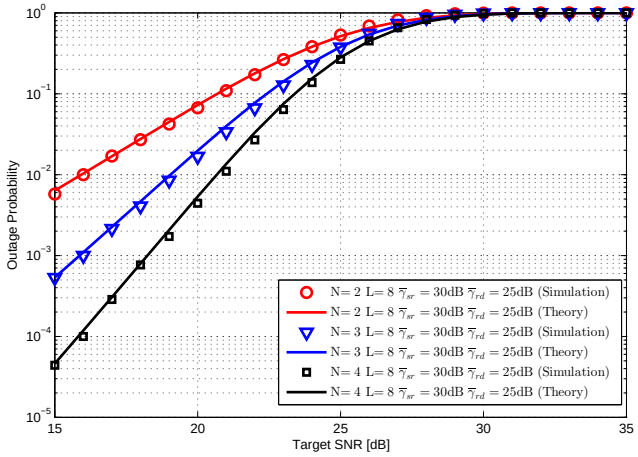


Fig. 5. Outage probability performance of the max-link scheme for different relay number $N$.

max-SNR schemes, the best outage performance is achieved in the symmetric channel. Moreover, the outage performance advantage of the AF max-link scheme over the traditional max-SNR scheme is also more significant in the symmetric than in the asymmetric channels. For example, when the target SNR=10dB, the outage probability differences between the max-link and max-SNR are approximately as large as 28dB for symmetric channels, and only about 2dB for asymmetric channels[6].

This can be explained as follows: In the AF max-link scheme, as is shown in (10), the outage performance depends on both the outage probability for every buffer state and the distributions of the buffer states, because different buffer states may correspond to different available links for the relay selection. On the one hand, the outage probability for a given buffer state is always minimized in the symmetric channel. This is because, as is shown in the outage bound in Section V-A, the outage probability for any buffer state depends on the minimum SNR of the source-to-relay and relay-to-destination channels, which is clearly minimized in the symmetric channels. On the other hand, if the channels become more asymmetric, the relay buffers are more likely to be full or empty, corresponding to fewer available links, which also deteriorates the outage performance.

In comparison, the traditional AF max-SNR scheme does not have buffer states and the available links for selection are always equal to the relay numbers. Thus the outage performance solely depends on the minimum SNR of the source-to-relay and relay-to-destination channels, and is optimum in symmetric channels. Therefore, when the channels become more asymmetric, there are two and one deteriorating factors in the outage performance for the max-link and max-SNR respectively, so that the outage performance of the max-link deteriorates faster than that of the max-SNR scheme. Therefore, compared with the traditional relay selection scheme, the buffer-aided max-link scheme is most effective in the

[6]Outage probability in dB = 10 log(outage probability)

symmetric channel configuration.

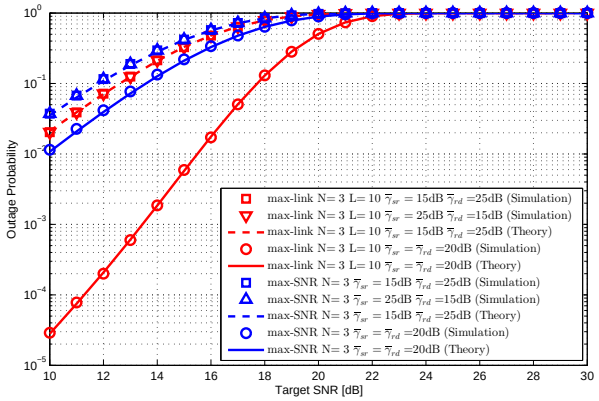


Fig. 6. Outage performance comparison between the AF max-link and max-SNR schemes with different channel configurations.

### C. Diversity order and coding gain

In order to show the diversity gain, Fig. 7 considers a symmetric channel configuration for which $\bar{\gamma}_{sr} = \bar{\gamma}_{rd} = 25$dB. As is proved in Section V, the diversity orders of the AF max-link scheme are $N$ and $2N$, when the buffer sizes are $L = 1$ and $L \to \infty$ respectively. On the other hand, the diversity order of the max-SNR is $N$. Therefore, the max-link schemes with $(N, L = 1)$ and $(N, L \to \infty)$ have the same diversity orders as those for the max-SNR with $N$ and $2N$ respectively, which is clearly verified in Fig. 7.

It is interesting to observe that, because of the coding gain, the max-link scheme with $(N = 5, L = 1)$ has significant better outage performance than the max-SNR scheme with $N = 5$, though they have the same diversity orders. Fig. 7 shows that, when SNR $= 14$dB, the outage probability difference between max-SNR with $N = 5$ and max-link with $(N = 5, L = 1)$ is approximately 11dB, which well matches the approximate coding gain obtained from (64) that is $10(N-1)\log 2 = 12$dB when $N = 5$.

On the other hand, for the max-link scheme $N = 5, L \to \infty$, the available link for every buffer state is $2N = 10$. Then following the similar procedure in Section V, we can obtain that the coding gain of the max-link with $N = 5, L \to \infty$ over the max-SNR with $2N = 10$ is approximately $10(2N-1)\log 2 = 27$dB. But Fig. 7 shows that, when SNR $= 14$dB, the outage probability difference between the max-SNR with $N = 10$ and max-link with $(N = 5, L \to \infty)$ is approximately 31dB, which well matches the analytical result.

## VIII. CONCLUSION

In this paper, we studied in detail the performance of the buffer-aided AF max-link relay selection scheme for both symmetric and asymmetric channels. We derived the closed form expressions for the outage probability of the proposed scheme. The results showed that the max-link scheme is most effective over the traditional max-SNR scheme when the source-to-relay and relay-to-destination links are symmetric. We also derived the average packet delay of the max-link scheme under both symmetric and asymmetric channel configurations. We proved that the diversity order of the AF max-link scheme is between $N$ and $2N$, where the lower and upper limits were obtained when the buffer size is 1 and $\infty$ respectively. We also analytically showed the coding gain of the max-link scheme over the traditional max-SNR scheme. Finally, extensive numerical simulations were given to verify the analyse in this paper.

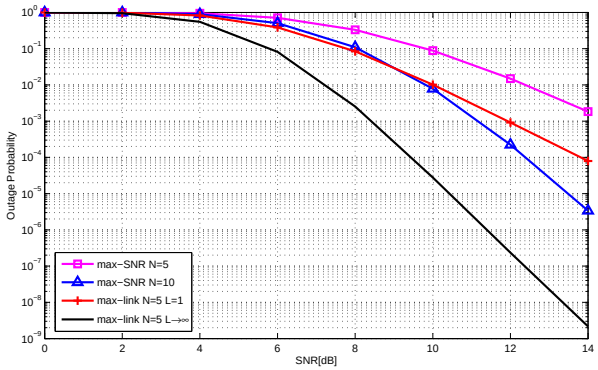


Fig. 7. Diversity order and coding gain of the AF max-link scheme.

## IX. ACKNOWLEDGEMENT

This work was supported in part by the Important National Science and Technology Specific Projects of China under Grant 2013ZX03001024.

The authors also thank the associate editor and five anonymous reviewers who have added much to the clarity of our papers.

## APPENDIX - PROOF OF (15)

Since the integration area of (14) is closed by the curve $\frac{\gamma_{th}(x+1)}{x-\gamma_{th}}$, $x \geq 0$ axis and $y \geq 0$ axis, the integration can be split into three parts as (65) in top of next page. Parts $A$ and $B$ can be obtained as

$$A = [1 - F_{\gamma_{R_k D}^{(s_j)}}(\gamma_{th})] F_{\gamma_{SR_k}^{(s_i)}}(\gamma_{th}), \quad B = F_{\gamma_{R_k D}^{(s_j)}}(\gamma_{th}), \tag{66}$$

respectively. Part $C$ is further divided into parts $C_1$ and $C_2$ as

$$C = \underbrace{\int_{\gamma_{th}}^{\infty} f_{\gamma_{R_k D}^{(s_j)}}(y) F_{\gamma_{SR_k}^{(s_i)}}[\frac{\gamma_{th}(y+1)}{y-\gamma_{th}}]\, dy}_{C_1} \underbrace{- [1 - F_{\gamma_{R_k D}^{(s_j)}}(\gamma_{th})] F_{\gamma_{SR_k}^{(s_i)}}(\gamma_{th})}_{C_2}. \tag{67}$$

Noticing $C_2$ is equal to $A$ in (66), we now need to calculate part $C_1$. First applying a binomial expansion for $F_{\gamma_{SR_k}^{(s_i)}}[\frac{\gamma_{th}(y+1)}{y-\gamma_{th}}]$ and $f_{\gamma_{R_k D}^{(s_j)}}(y)$ yields (68) and (69) in the top of next page, respectively. Substituting (68) and (69) back into $C_1$ yields (70). Noticing $C_{11}$ is actually equal to $1 - B$ as is shown in (66).

Finally, substituting $A$, $B$ and $C$ back into (67) gives (15). ■

$$P(\gamma_D^{(s_i,s_j)} \le \gamma_{th}) = \underbrace{\int_{\gamma_{th}}^{\infty}\int_{0}^{\gamma_{th}} f_{\gamma_{SR_k}^{(s_i)}\gamma_{R_kD}^{(s_j)}}(x,y)\,dx\,dy}_{A} + \underbrace{\int_{0}^{\gamma_{th}}\int_{0}^{\infty} f_{\gamma_{SR_k}^{(s_i)}\gamma_{R_kD}^{(s_j)}}(x,y)\,dx\,dy}_{B} + \underbrace{\int_{\gamma_{th}}^{\infty}\int_{\gamma_{th}}^{\frac{\gamma_{th}(y+1)}{y-\gamma_{th}}} f_{\gamma_{SR_k}^{(s_i)}\gamma_{R_kD}^{(s_j)}}(x,y)\,dx\,dy}_{C}. \tag{65}$$

$$F_{\gamma_{SR_k}^{(s_i)}}\left[\frac{\gamma_{th}(y+1)}{y-\gamma_{th}}\right] = \underset{(m,n)=(0,0)}{1} + \sum_{\substack{m=0\\(m,n)\neq(0,0)}}^{K_{sr}^{(s_i)}}\sum_{n=0}^{K_{rd}^{(s_i)}} C_{K_{sr}^{(s_i)}}^{m} C_{K_{rd}^{(s_i)}}^{n}\cdot(-1)^{m+n} e^{-\left(\frac{m}{\bar{\gamma}_{sr}}+\frac{n}{\bar{\gamma}_{rd}}\right)\cdot\frac{\gamma_{th}(y+1)}{y-\gamma_{th}}}. \tag{68}$$

$$f_{\gamma_{R_kD}^{(s_j)}}(y) = \sum_{a_1=0}^{K_{sr}^{(s_j)}-1}\sum_{a_2=0}^{K_{rd}^{(s_j)}} C_{K_{sr}^{(s_j)}-1}^{a_1} C_{K_{rd}^{(s_j)}}^{a_2}(-1)^{a_1+a_2}\frac{K_{sr}^{(s_j)}}{\bar{\gamma}_{sr}} e^{-M_1 y} + \sum_{a_3=0}^{K_{rd}^{(s_j)}-1}\sum_{a_4=0}^{K_{sr}^{(s_j)}} C_{K_{rd}^{(s_j)}-1}^{a_3} C_{K_{sr}^{(s_j)}}^{a_4}(-1)^{a_3+a_4}\frac{K_{rd}^{(s_j)}}{\bar{\gamma}_{rd}} e^{-M_2 y}. \tag{69}$$

$$\begin{aligned} C_1 = \underbrace{[1-F_{\gamma_{R_kD}^{(s_j)}}(\gamma_{th})]}_{C_{11}} &+ \sum_{\substack{m\\(m,n)\neq(0,0)}}^{K_{sr}^{(s_i)}}\sum_{n}^{K_{rd}^{(s_i)}} C_{K_{sr}^{(s_i)}}^{m} C_{K_{rd}^{(s_i)}}^{n}(-1)^{m+n} 2e^{-M_4\gamma_{th}}\sqrt{M_4 M_{\gamma_{th}}} \\ &\cdot\Big[\frac{K_{sr}^{(s_j)}}{\bar{\gamma}_{sr}}\sum_{a_1=0}^{K_{sr}^{(s_j)}-1}\sum_{a_2=0}^{K_{rd}^{(s_j)}}(-1)^{a_1+a_2} C_{K_{sr}^{(s_j)}-1}^{a_1} C_{K_{rd}^{(s_j)}}^{a_2}\frac{e^{-M_1\gamma_{th}}}{\sqrt{M_1}}\mathcal{B}(1,2\sqrt{M_1 M_4 M_{\gamma_{th}}}) \\ &+\frac{K_{rd}^{(s_j)}}{\bar{\gamma}_{rd}}\sum_{a_3=0}^{K_{rd}^{(s_j)}-1}\sum_{a_4=0}^{K_{sr}^{(s_j)}}(-1)^{a_3+a_4} C_{K_{rd}^{(s_j)}-1}^{a_3} C_{K_{sr}^{(s_j)}}^{a_4}\frac{e^{-M_2\gamma_{th}}}{\sqrt{M_2}}\mathcal{B}(1,2\sqrt{M_2 M_4 M_{\gamma_{th}}})\Big] \end{aligned} \tag{70}$$

where

$$M_1 = \frac{1}{\bar{\gamma}_{sr}} + \frac{a_1}{\bar{\gamma}_{sr}} + \frac{a_2}{\bar{\gamma}_{rd}}, M_2 = \frac{1}{\bar{\gamma}_{rd}} + \frac{a_3}{\bar{\gamma}_{rd}} + \frac{a_4}{\bar{\gamma}_{sr}}, M_4 = \frac{m}{\bar{\gamma}_{sr}} + \frac{n}{\bar{\gamma}_{rd}}, M_{\gamma_{th}} = \gamma_{th}(\gamma_{th}+1). \tag{71}$$

## REFERENCES


[1] W. Su and X. Liu, "On optimum selection relaying protocols in cooperative wireless networks," *IEEE Trans. Wireless Commun.*, vol. 58, pp. 52–57, Jan. 2010.

[2] A. Bletsas, A. Khisti, D. P. Reed, and A. Lippman, "A simple cooperative diversity method based on network path selection," *IEEE J. Sel. Areas Commun.*, vol. 24, pp. 659–672, March 2006.

[3] A. Ikhlef, D. S. Michalopoulos, and R. Schober, "Buffers improve the performance of relay selection," *in Proc. 2011 IEEE Global Commun. Conf, Houston,Texas,USA*, pp. 1–6, Dec. 2011.

[4] I. Krikidis, T. Charalambous, and J. S. Thompson, "Buffer-aided relay selection for cooperative diversity systems without delay constraints," *IEEE Trans. Wireless Commun.*, vol. 11, no. 5, pp. 1957–1967, May 2012.

[5] H. Liu, P. Popovski, E. Carvalho, and Y. Zhao, "Sum-rate optimization in a two-way relay network with buffering," *IEEE Commun. Letters*, vol. 17, pp. 95–98, Jan. 2013.

[6] A. Ikhlef, D. S. Michalopoulos, and R. Schober, "Max-max relay selection for relays with buffers," *IEEE Trans. Wireless Commun.*, vol. 11, no. 3, pp. 1124–1135, May 2012.

[7] N. Zlatanov, R. Schober, and L. Lampe, "Buffer-aided relaying in a three node network," *in Proc. 2012 IEEE International Symposium on Information Theory Proceedings,Cambridge,Massachusetts,USA*, pp. 781–785, July 2012.

[8] N. Zlatanov, R. Schober, and P. Popovski, "Buffer-aided relaying with adaptive link selection," *IEEE J. Sel. Areas Commun.*, vol. 31, pp. 1530–1542, Aug. 2013.

[9] N. Zlatanov, R. Schober, and P. Popovski, "Buffer-aided relaying with adaptive link selection-fixed and mixed rate transmission," *IEEE Trans. Inform. Theory*, vol. 59, pp. 2816–2840, May 2013.

[10] G. Chen, Z. Tian, Y. Gong, and J. A. Chambers, "Decode-and-forward buffer-aided relay selection in cognitive relay networks," *IEEE Trans. Veh. Technology*, Mar. 2014.

[11] G. Chen, Z. Tian, Y. Gong, Z. Chen, and J. A. Chambers, "Max-ratio relay selection in secure buffer-aided cooperative wireless networks," *IEEE Trans. inform. Forensics and Security.*, vol. 9, pp. 719–729, Apr. 2014.

[12] B. Barua, H. Q. Ngo, and H. Shin, "On the sep of cooperative diversity with opportunistic relaying," *IEEE Commun. Letters*, vol. 12, pp. 727–729, Oct. 2008.

[13] I. Krikidis, J. S. Thompson, S. McLaughlin, and N. Goertz, "Amplify-and-forward with partial relay selection," *IEEE Commun. Letters*, vol. 12, pp. 235–237, Apr. 2008.

[14] H. A. Suraweera, M. Soysa, C. Tellambura, and H. K. Garg, "Performance analysis of partial relay selection with feed back delay," *IEEE Signal Process. Lett*, vol. 17, pp. 531–534, June 2010.

[15] W. J. Huang, Y. W. Hong, and C. C. J. Kuo, "Lifetime maximization for amplify-and-forward cooperative networks," *IEEE Trans. Wireless Commun.*, vol. 7, pp. 1800–1805, May 2008.

[16] I. Krikidis, J. S. Thompson, S. McLaughlin, and N. Goertz, "Max-min relay selection for legacy amplify-and-forward systems with interference," *IEEE Trans. Wireless Commun.*, vol. 8, pp. 3016–3027, June 2009.

[17] H. A. David, "Order statistics second edition," *John Wiley Sons Ltd*, 1981.

[18] M. Abramowitz and I. A. Stegun, "Handbook of mathematical functions: with formulas, graphs, and mathematical tables," *New York: Dover*, 1965.

[19] C. M. Grinstead and J. L. Snell, "Introduction to probability: Second revised edition," *American Mathematical Society*, 1991.

[20] J. R. Norris, "Markov chains," *Cambridge University Press*, 1998.

[21] A. Berman and R. J. Plemmons, "Nonnegative matrices in the mathematical sciences," *Society of industrial and applied mathematics*, 1994.

[22] J. N. Laneman, D. N. C. Tse, and G. W. Wornell, "Cooperative diversity in wireless networks: Efficient protocols and outage behavior," *IEEE Trans. Inform. Theory*, vol. 50, pp. 3062–3080, Dec. 2004.

[23] J. D. C. Little and S. C. Graves, "Little's law," *International Series*

*in Operations Research & Management Science*, vol. 115, pp. 81–100, 2008.

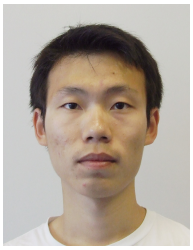

**Zhao Tian** (S'12) received the B. Eng. degree in School of Electronic, Electrical and Systems Engineering from Loughborough University, UK, in 2012 He is currently working toward the Ph.D. degree in Advanced Digital Signal Process Group in School of Electronic, Electrical and Systems Engineering from Loughborough University, UK with full postgraduate scholarship from Engineering and Physical Sciences Research Council (EPSRC). His current research interest include the general field of wireless communications with emphasis on buffer-aided relaying.

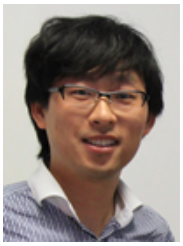

**Gaojie Chen** (S'09-M'12) received the B. Eng. and B. Ec. in Electrical Information Engineering and International Economics and Trade from the Northwest University, Shaanxi, China, in 2006, and the M.Sc (Distinction) and Ph.D degrees from Loughborough University, Loughborough, UK, in 2008 and 2012, respectively, all in Electrical and Electronic Engineering. From 2008 to 2009 he worked, as a software engineering in DTmobile, Beijing, China, and from 2012 to 2013 as a Research Associate in the School of Electronic, Electrical and Systems Engineering at the Loughborough University, Loughborough, UK. He is currently a Research Fellow in the Faculty of Engineering and Physical Sciences at the University of Surrey, Guildford, UK. His current research interests include information theory, wireless communications, cooperative communications, cognitive radio and secrecy communications.

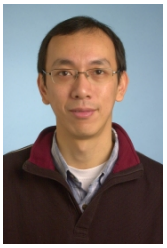

**Yu Gong** is with School of Electronic, Electrical and Systems Engineering, Loughborough University, UK, in July 2012. Dr Gong obtained his BEng and MEng in electronic engineering in 1992 and 1995 respectively, both at the University of Electronics and Science Technology of China. In 2002, he received his PhD in communications from the National University of Singapore. After PhD graduation, he took several research positions in Institute of Inforcomm Research in Singapore and Queen's University of Belfast in the UK respectively. From 2006 and 2012, Dr Gong had been an academic member in the School of Systems Engineering, University of Reading, UK. His research interests are in the area of signal processing and communications including wireless communications, cooperative networks, non-linear and non-stationary system identification and adaptive filters.

**Zhi Chen** (M'04) received B. Eng, M. Eng., and Ph.D. degree in Electrical Engineering from University of Electronic Science and Technology of China (UESTC), in 1997, 2000, 2006, respectively, all in electrical engineering. After his Ph.D. graduation, he joined the National Key Lab of Science and Technology on Communications, UESTC, where he was promoted to Professor in August 2013.. He was a visiting scholar at University of California, Riverside during 2010-2011. His current research interests include wireless communication and signal processing, specifically relay and cooperative communications, interference coordination and cancellation. Dr. Chen has served as a reviewer for various international journals and conferences, including IEEE Transactions on Signal Processing, IEEE Transactions on Vehicular Technology, and many more.

**Jonathon A. Chambers** (S'83-M'90-SM'98-F'11) received the Ph.D. and DSc degrees in signal processing from the Imperial College of Science, Technology and Medicine (Imperial College London), London, U.K., in 1990 and 2014. From 1991 to 1994, he was a Research Scientist with the Schlumberger Cambridge Research Center, Cambridge, U.K. In 1994, he returned to Imperial College London, as a Lecturer in signal processing and was promoted as a Reader (Associate Professor) in 1998. From 2001 to 2004, he was the Director of the Centre for Digital Signal Processing and a Professor of signal processing with the Division of Engineering, King's College London, London. From 2004 to 2007, he was a Cardiff Professorial Research Fellow with the School of Engineering, Cardiff University, Wales, U.K. In 2007, he joined the Department of Electronic and Electrical Engineering, Loughborough University, Loughborough, U.K., where he heads the Advanced Signal Processing Group and serves as the Associate Dean (Research) for Loughborough University in London. He is a coauthor of the books Recurrent Neural Networks for Prediction: Learning Algorithms, Architectures and Stability (New York, NY, USA: Wiley, 2001) and EEG Signal Processing (New York, NY, USA: Wiley, 2007). He has advised more than 50 researchers through to Ph.D. graduation and published more than 350 conference proceedings and journal articles, many of which are in IEEE journals. His research interests include adaptive and blind signal processing and their applications. Dr. Chambers is a Fellow of the Royal Academy of Engineering, U.K., and the Institution of Electrical Engineers (IEE). He was the Technical Program Chair of the 15th International Conference on Digital Signal Processing and the 2009 IEEE Workshop on Statistical Signal Processing, both held in Cardiff, U.K., and a Technical Program Cochair for the 36th IEEE International Conference on Acoustics, Speech, and Signal Processing, Prague, Czech Republic. He received the first QinetiQ Visiting Fellowship in 2007 for his outstanding contributions to adaptive signal processing and his contributions to QinetiQas a result of his successful industrial collaboration with the international defense systems company QinetiQ. He has served on the IEEE Signal Processing Theory and Methods Technical Committee for six years, the IEEE Signal Processing Society Awards Board for three years and is currently a member of the IEEE Signal Processing Conference Board, and the European Signal Processing Society Best Paper Awards Selection Panel. He has also served as an Associate Editor of the IEEE TRANSACTIONS ON SIGNAL PROCESSING for three terms over the periods 1997-1999, 2004-2007, and 2011- (and is currently a Senior Area Editor).